

## **General Disclaimer**

### **One or more of the Following Statements may affect this Document**

- This document has been reproduced from the best copy furnished by the organizational source. It is being released in the interest of making available as much information as possible.
- This document may contain data, which exceeds the sheet parameters. It was furnished in this condition by the organizational source and is the best copy available.
- This document may contain tone-on-tone or color graphs, charts and/or pictures, which have been reproduced in black and white.
- This document is paginated as submitted by the original source.
- Portions of this document are not fully legible due to the historical nature of some of the material. However, it is the best reproduction available from the original submission.

NASA Technical Memorandum 79255

(NASA-TM-79255) CHARACTERISTICS OF PRIMARY  
ELECTRIC PROPULSION SYSTEMS (NASA) 17 p  
HC A02/MF A01 CSCL 21C

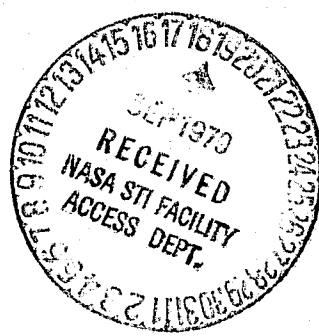
N79-30290

Unclassified  
G3/20 31862

## CHARACTERISTICS OF PRIMARY ELECTRIC PROPULSION SYSTEMS

David C. Byers  
Lewis Research Center  
Cleveland, Ohio

Prepared for the  
Fourteenth International Conference on Electric Propulsion  
sponsored by the American Institute at Aeronautics and Astronautics  
and Deutsche Gesellschaft fur Luft- und Raumfahrt  
Princeton, New Jersey, October 31-November 2, 1979



CHARACTERISTICS OF PRIMARY ELECTRIC PROPULSION SYSTEMS

David C. Byers\*  
 National Aeronautics and Space Administration  
 Lewis Research Center  
 Cleveland, Ohio

Abstract

The use of advanced electric propulsion systems will provide cost and performance benefits for future energetic space missions. A methodology to predict the characteristics of advanced electric propulsion systems was developed and programmed for computer calculations to allow evaluation of a broad set of technology and mission assumptions. The impact on overall thrust system characteristics was assessed for variations of propellant type, total accelerating voltage, thruster area, specific impulse, and power system approach. The data may be used both to provide direction to technology emphasis and allow for preliminary estimates of electric propulsion system properties for a wide variety of application.

Nomenclature

$A$	active ion acceleration area of thruster, $\text{m}^2$	$N$	total number of thrusters
$A_{TH}$	radiator plan area, $\text{m}^2$	$N'$	integral number of active thrusters
$EX$	number of redundant thrusters	$N''$	initial number of active thrusters
$F_V$	transmission line factor	$P$	input power to interface module, kW
$G$	load on propellant tank in units of g	$P_B$	individual thruster beam power, kW
$g$	gravitational constant, $9.8 \text{ m-sec}^{-2}$	$P_C$	housekeeping converter output power, kW
$I_{SP}$	specific impulse, sec	$P_D$	individual thruster discharge power, kW
$L$	transmission line length, m	$P_{DI}$	distribution inverter output power, kW
$M$	propellant ion mass, AMU	$P_{DIS}$	dissipated power, kW
$M_B$	beam power supply mass, kg	$P_F$	individual thruster fixed power, kW
$M_C$	housekeeping converter mass, kg	$P_{LB}$	beam supply dissipated power, kW
$M_D$	discharge power supply mass, kg	$P_{LC}$	housekeeping converter dissipated power, kW
$M_{DI}$	distribution inverter mass, kg	$P_{LD}$	discharge supply dissipated power, kW
$M_F$	final spacecraft dry mass, kg	$P_{LDI}$	distribution inverter dissipated power, kW
$M_{GT}$	total gimbal mass, kg	$P_{LO}$	low voltage supply dissipated power, kW
$M_{IM}$	interface module structural mass less structural mass, kg	$P_{LOSS}$	transmission line dissipated power, kW
$M_{IMS}$	interface module structural mass, kg	$P_{LRU}$	reconfiguration unit dissipated power, kW
$M_L$	transmission line mass, kg	$P_{LTSC}$	thrust system controller dissipated power, kW
$M_{LO}$	low power supply mass, kg	$P_P$	propellant storage pressure, Pa
$M_P$	propellant mass, kg	$P_{RU}$	reconfiguration unit output power, kW
$M_{RU}$	reconfiguration unit mass, kg	$P_{SYS}$	input power to transmission line, kW
$M_T$	propellant tank mass, kg	$R$	ratio of net to total accelerating voltage
$M_{TH}$	thermal control system mass, kg	$S$	allowable stress in propellant tank walls, Pa
$M_{TM}$	thrust module mass, kg	$T$	individual thruster output thrust, N
$M_{TMS}$	thrust module structure mass, kg	$T_T$	thrust module output thrust, N
$M_{TS}$	thruster mass, kg	$\Delta T$	thrusting time, days
$M_{TSC}$	thrust system controller mass, kg	$V_B$	net accelerating voltage, V
$M_{TST}$	total thruster mass, kg	$V_L$	transmission line voltage, V
		$V_M$	mission velocity increment, $\text{m-sec}^{-1}$
		$\Delta V$	total accelerating voltage, V
		$X$	propellant tank design margin
		$a_{PS}$	specific mass of power source, $\text{kg-w}^{-1}$
		$a_{HR}$	specific mass of transmission line thermal control system, $\text{kg-w}^{-1}$
		$\gamma$	thrust loss factor
		$ev$	energy required to form an ampere of ion beam, W/A
		$\rho_{AR}$	density of liquid argon, $\text{kg-m}^{-3}$
		$\rho_L$	density of transmission line, $\text{kg-m}^{-3}$
		$\rho_P$	propellant density, $\text{kg-m}^{-3}$
		$\rho_T$	propellant tank material density, $\text{kg-m}^{-3}$
		$\eta_U$	propellant utilization efficiency
		$\Omega_L$	resistivity of transmission line, ohm-m

\*Head, Electric Thruster Section Member AIAA

## Introduction

Electron bombardment ion thruster systems are approaching operational application. In the United States both auxiliary<sup>(1)</sup> and primary<sup>(2)</sup> ion propulsion are in advanced stages of development. The auxiliary system utilizes 8-cm<sup>(3)</sup> mercury thrusters and is presently scheduled for a flight test on the Air Force P80-1 satellite. The primary system employs 30-cm mercury thrusters and plans<sup>(4)</sup> are to achieve technology readiness of that system by 1981. In addition, both Germany<sup>(5)</sup> and Japan<sup>(6)</sup> have made plans to space test auxiliary propulsion concepts which use 10 and 5-cm mercury thrusters, respectively.

Auxiliary propulsion thrusters under development produce thrusts between about 2 and 10 mN. These thrusters were designed for spacecraft with masses up to about 2500 kg. The design of the 30-cm thruster system was greatly influenced by planetary mission requirements. Such missions are usually power limited and quite performance sensitive and, as such, strongly drive the propulsion system design in areas such as efficiency and power throttling requirements.

With the advent of the Shuttle, new and greatly expanded missions will become possible. Examples are very large communications systems,<sup>(7)</sup> space manufacturing facilities,<sup>(8)</sup> and a variety of other large space systems.<sup>(9)</sup> It is likely that for many such missions the electric propulsion concepts systems now in final development will not be optimal or appropriate based on technical or cost considerations. It is probable that the use of advanced technologies could strongly benefit the more energetic future missions. These technologies include alternate propellants, such as inert gases;<sup>(10)</sup> larger thrusters;<sup>(11)</sup> operation at increased thrust and/or power densities;<sup>(12)</sup> and improved Power Management and Control (PMAC) concepts.<sup>(13)</sup>

It is the intent of this paper to describe the characteristics of electron bombardment ion thruster systems for a broad range of mission and propulsion technology assumptions. A methodology was previously presented<sup>(14)</sup> which defined the elements of a thrust system, parametrically described the characteristics of those elements, and then defined the overall system properties. Two point system designs were presented in Ref. 14 to provide insight into the use of the overall methodology.

The element descriptions in Ref. 14 were subsequently generalized to allow convenient updating as new technologies and information becomes available. In addition, a computer code was completed so that system characteristics could be rapidly defined for a large range of propulsion element and mission characteristics. This paper will present the initial results of use of the computer code in order to allow technologists to evaluate the impact of various technology advances and provide mission planners with preliminary estimates of the characteristics of electron-bombardment ion thruster systems.

## System Approach

A thrust system was assumed to consist of a thrust module, an interface module, and a power transmission line. The elements contained in each of the three subsystems are shown in Fig. 1. This

system approach has been used previously<sup>(15)</sup> and is convenient for parametric evaluation of a thrust system. The methodology used to describe the overall system was presented in detail in Ref. 14 and will only be summarized herein. Briefly, the individual elements of the system were defined in parametric fashion. Element properties, such as thruster output power, mass, and thrust could be calculated after the input parameters, such as thruster size, propellant type, and specific impulse were selected. Detailed system designs<sup>(16)</sup> were used to obtain values for structural and thermal control system masses and radiator areas. After certain mission parameters were selected, the methodology allowed each subsystem to be independently defined, interfaced with the other subsystems, and finally provided values for the overall system properties. In the following sections the properties of all system elements will be described followed by initial results of a computer code constructed to predict system properties.

## Mission Parameters

The system thrust is obtained from:

$$T_T = \frac{M_F}{\Delta T} \left( e^{\frac{V_M}{I_{SP}^g}} - 1 \right) (I_{SP}^g) 1.16 \times 10^{-5} \quad (1)$$

all symbols are defined in the nomenclature section.

The propellant mass is given by:

$$M_P = M_F \left( e^{\frac{V_M}{I_{SP}^g}} - 1 \right) \quad (2)$$

The variables on the right hand side of Eq. 1 are all inputs to the computer program. The thrust, and the subsequently defined thrust system, may be defined for a variety of primary and auxiliary propulsion functions if the term  $\Delta T$  is taken to be thrusting time and the mission velocity increment is appropriately selected.

## Element Descriptions

Details of the parametric descriptions of all system elements were presented in Ref. 14 and the same approaches will be used in this paper unless otherwise noted. For completeness, a brief summary of the technique used to describe each element will be presented below and the reader is referred to Ref. 14 for more detailed information.

## Thruster

Performance. Following Ref. 14 the thrust per unit area of accelerator grid given by:

$$\frac{T}{A} = (r) (5.2 \times 10^{-9}) \frac{V_B^{2.75}}{R^{2.25}} \quad (3)$$

and the input thruster power per unit area of accelerator grid described by:

$$\frac{P_T}{A} = \frac{3.6 \times 10^{-8}}{\sqrt{M}} \left( \frac{V_B}{R} \right)^{2.25} (V_B + \epsilon v) + \frac{P_F}{A} \quad (4)$$

As stated in Ref. 14, the magnitudes of the thrust and power densities given in Eqs. (3) and (4), respectively, are 90 percent of limit values presented in the literature.(17) The values of the constants in Eqs. (3) and (4) are taken from Ref. 14. The computer code used for system calculations allowed variation of all constants used in equations describing elements. This feature allows element properties to be easily changed as new information becomes available. Table I lists certain thruster performance parameters for four candidate propellants. The values shown on Table I have been achieved previously and may also be easily varied in the computer code as performance improvements occur.

Number of thrusters. The thrust output of an individual thruster is obtained by multiplying Eq. (3) by the assumed active ion accelerating area of the thruster. The number of active thrusters is obtained from:

$$N'' = \frac{T_T}{T} \quad (5)$$

The number of active thrusters obtained from Eq. (5) will not, in general, be an integral number. The computer code calculates the final number of active thrusters,  $N'$ , by rounding  $N''$  up to the next highest integral number. In Ref. 14 the value of system thrust and trip time were adjusted so that all active thrusters were operated at the full thrust and power implied by Eqs. (3) and (4), respectively. This step was not taken in the calculations presented herein and the final system thrust remained as given by Eq. (1) for the assumed trip time, specific impulse, and final dry mass. In general, this procedure results in two of the active thrusters operating at slightly less than full power. The power processor masses and low power requirements of the throttled thrusters were, however, assumed to be equal to those of a thruster operating at full power. The approach used in this paper was selected as it allowed rapid convergence of computer calculations of system parameters such as trip time or final dry mass.

The total number of thrusters,  $N$ , is obtained by assuming some number of redundant, standby, thrusters,  $EX$ . The total number of thrusters is then given by:

$$N = N' + EX \quad (6)$$

Mass. Individual thruster mass as a function of active accelerator grid diameter was given in Fig. 4 of Ref. 14. Those data may be expressed by the following equation for circular thrusters:

$$M_{TS} = 2.4 + 4.24 A + 3[7.9(A)^{0.5} + 1.13 \times 10^{-1} A] \quad (7)$$

The total thruster mass is then given by:

$$M_{TST} = N M_{TS} \quad (8)$$

Dissipated power. The dissipated powers of system elements are important because the thermal control system must be sized accordingly. The thruster does not, however, require a thermal control system as the dissipated power is radiated to space from the thruster itself.(18)

### Gimbal

The total gimbal mass will be assumed to remain at the fraction of thruster mass defined in a detailed point system design(16) as:

$$M_{GT} = 0.34 M_{TST} \quad (9)$$

The gimbals are powered only when active gimbaling occurs and the dissipated power will therefore be considered negligible.

### Propellant Distribution

From Ref. 14 a mass of one kilogram per thruster will be charged to the propellant distribution system.

### Thrust Module Structure

The thrust module structure serves to cantilever the thrusters and gimbals away from the interface module. This structure mass was calculated in the point system design of Ref. 16 and it will be assumed to be the same fraction of the sum of thruster and gimbal mass as given therein:

$$M_{TMS} = 0.31(M_{TST} + M_{GT}) \quad (10)$$

### Power Management and Control

The Power Management and Control (PMAC) system is comprised of the beam, discharge, and low power supplies in the thrust module and the beam and discharge reconfiguration unit, the distribution inverter, the converter, and the thrust system controller located in the interface module.

In Ref. 14 both conventional and Alternating Current (AC) PMAC systems were evaluated. The conventional PMAC system is designed to accept DC power provided by a solar array while the AC system used 1200 Hz power for the beam and discharge supplies. Details of the PMAC systems are discussed in Ref. 14 and Tables II and III show the assumed masses and dissipated powers for all PMAC elements for both approaches. With two exceptions all values shown on Tables II and III are the same as in Ref. 14. The low power supply mass was assumed to be 8 kg, instead of 15, based on recent data(19) which indicate significant reduction in low power supply mass is possible. In addition, the total power dissipated in the beam and discharge supplies was made proportional to  $N''$  rather than  $N'$ . This change was made to be consistent with the modified method of specifying thrust discussed previously. As shown on Table II, all thrusters, including redundant ones, were assumed to have a full complement of beam, discharge, and low power supplies. In addition one each redundant distribution inverter, housekeeping converter, and thrust system controller was also assumed.

### Thermal Control System

The thermal control system was assumed to use heat pipe radiators and reject heat from only one side. The masses and areas were taken from Ref. 16 and were sized to maintain baseplate temperatures

at 323° K. From Ref. 16 the mass and area of the thermal control system are given by:

$$M_{TH} = 31 P_{DIS} \quad (11)$$

and

$$A_{TH} = 2.86 P_{DIS} \quad (12)$$

### Propellant Tankage

Both pressurized noncryogenic and cryogenic propellant tank concepts were evaluated in Ref. 14. Spherical pressurized tank masses were calculated for both Xenon and Mercury propellants and given by:

$$\frac{M_T}{M_P} = \frac{3}{2} \frac{\rho_T X}{\rho_P S} \left[ P_P + G \left( \frac{M_P}{2\pi} \right)^{1/3} \left( \frac{4}{3} \rho_P \right)^{2/3} \right] \quad (13)$$

If a small cylindrical section exists in a basically spherical tank, Eq. (13) may be used if the left hand term in the bracket is doubled to account for axial loads.

The tankage mass fractions of cryogenic tanks were based on a detailed point design for an Argon tank(20) which was modified to account for other propellants in Ref. 14 as:

$$\left( \frac{M_T}{M_P} \right)_{CRY} \approx \frac{\rho_{AR}}{\rho_P} (M_P)^{-1/3} \quad (14)$$

### Interface Module Structure

From Ref. 14 the interface module structure is assumed to be:

$$M_{IMS} = 0.04 (M_{TM} + M_{IM}) \quad (15)$$

The value of interface module structure was taken to be about three times that calculated in a detailed point design for a mercury thrust system.(16) This was done to provide design margin for systems which may be less compact than the design of Ref. 16.

### Transmission Subsystem

From Ref. 14 the mass and dissipated power in the transmission line are given as:

$$M_L = \frac{10^3 F_{VPL}}{V_L} \left[ n_L \rho_L (\alpha_{PS} + \alpha_{HR}) \right]^{1/2} \quad (17)$$

and

$$P_{LOSS} = \frac{LF_V}{V_L} \sqrt{\frac{\Omega_L \rho_L}{\alpha_{PS} + \alpha_{HR}}} \quad (18)$$

Representative values of  $F_V$ , line material, and heat rejection properties are given in Ref. 14.

### Thrust System Descriptions

This section will present the initial results of calculations of the characteristics of thrust systems using a computer program which used the methodology presented in Ref. 14. All calculations used the thruster performance data of Table I, the propellant tank parameters of Ref. 14, the PMAC characteristics shown on Tables II and III, and the numbers of redundant thrusters was fixed at two.

The effect of the variation of selected system and mission parameters will be presented. The results are presented for the several cases shown on Table IV which shows the major input parameters assumed for each case.

In all figures in this report the thrust system mass is the sum of the system dry mass and the propellant mass and represents the mass that must be transported to Low Earth Orbit or to the satellite operating orbit to perform orbit transfer or auxiliary propulsion functions, respectively. The system power is always defined as that at the input to the transmission line. The number of active thrusters shown on all figures is the value obtained directly from Eq. (5) and is generally not an integral number. This value was selected to avoid unevenness in the data which results when the final integral number of active thrusters (obtained as described previously) used to define system characteristics was plotted. As shown on Table IV, all plots presented herein assume, unless otherwise stated, a fixed final mass of  $10^4$  kg, a thrusting time of 150 days, and a mission velocity increment of  $6 \times 10^3$  m-sec $^{-1}$ . The final mass includes the payload (which is assumed to include the power source) and the dry thrust system mass. The mission velocity increment is about that of an orbit transfer from Shuttle to geosynchronous orbit.

### Total Accelerating Voltage

The thrust and power densities of bombardment ion thrusters are strongly influenced by the value of total accelerating voltage,  $\Delta V$ , at which the thruster is operated. Mercury ion thrusters, with close spaced ion optics, were operated(12) at values of  $\Delta V$  up to about 3 kV. For conservatism, the baseline case assumed in this paper will be a  $\Delta V$  of 2 kV.

The influence of  $\Delta V$  on thruster operation is shown in Fig. 2 where the output thrust of a 50-cm mercury thruster is shown as a function of specific impulse. Similar curves may be plotted to describe thruster input power.(14) The range of specific impulse shown for each  $\Delta V$  is specified by the range of the net to total accelerating voltage,  $R$ , over which thruster operation is assumed possible. Values of  $R$  between about 0.2 and 0.9 were demonstrated with three grid ion optics in Ref. 12 and this range will be assumed as the baseline in this paper. It should be noted that thrusters may be operated at values of  $R$ , and therefore specific impulse, beyond the limits shown on Fig. 2. Such operation will, however, cause strong reductions in thrust and power density from those values given in Eqs. (3) and (4), respectively.(14)

Figure 2 shows that at a fixed specific impulse the thrust from an individual thruster increases by between a factor of 3 and 4 as  $\Delta V$  in-

creases from 1.5 to 2.5 kV. Over the same variation of  $\Delta V$ , the limits assumed for  $R$  cause an increase of about 30 percent in the minimum and maximum achievable values specific impulse.

The effect of  $\Delta V$  on major system characteristics is shown on Fig. 3 and Table V shows details of element properties as  $\Delta V$  was varied. Due to the assumptions of fixed specific impulse and mission parameters the propellant mass and thrust are constant for the  $\Delta V$  variation and the major effect of variation of  $\Delta V$  between 1.5 to 2.5 kV was to change the number of active thrusters from about 18 to 6. The number of redundant thrusters was assumed to be 2 in all cases and, therefore, the total number of thrusters ranged from 20 to 8. Figure 3 shows that the system mass decreased by about 15 percent as  $\Delta V$  increased from 1.5 to 2.5 kV. That variation was entirely due to the approximate 40 percent reduction in system dry mass. Inspection of Table V indicates that nearly all of the dry mass decrease occurred in the thrust module. Decreasing the number of thrusters caused large decreases in the total masses of the thrusters; gimbals; beam, discharge, and low power supplies; and the thrust module structure. The system power varied by only about one percent for the  $\Delta V$  variation shown on Fig. 3 and that difference was primarily due to the power supplied to the low power supplies which basically varies directly with the number of thrusters.

It is clear from Fig. 3 that at a fixed specific impulse it is desirable to operate at as high a value of  $\Delta V$  as is consistent with thruster lifetime and stability. On the other hand, Fig. 2 shows that the value of  $\Delta V$  selected impacts the range of attainable specific impulse. For missions for which the specific impulse is a predominate cost or performance driver, the desired value of  $\Delta V$  may well be less than that determined from thruster operational criteria.

The variation in system dry mass of about 900 kg shown on Fig. 3 would be expected to influence the cost of the mission somewhat. It is likely, however, that the major impacts of the large variation in the number of thrusters would be on the cost of the thrust system hardware and in the system layout approach which would be conveniently placed in the Shuttle.

#### Specific Impulse

The effect of specific impulse on major system characteristics is shown on Figs. 4, 5, and 6 for mercury, xenon, and argon propellants, respectively. The total accelerating voltage was assumed to be 2 kV for all the propellants cases shown.

The range of specific impulse varied, as described previously, with propellant type and the ratio of the highest to lowest specific impulse was fixed at about 2.1 due to the constraint of operation at values of  $R$  between 0.2 and 0.9.

Figures 4, 5, and 6 show that the system mass decreased strongly with increasing specific impulse and that in all cases the decrease was primarily due to the reduction of propellant mass (The propellant mass, as expected, varied in a fashion inversely proportional to specific impulse). The fractional reduction of system mass with increasing specific impulse varied from about a factor of two with mer-

cury to about 30 percent with argon. This difference in system mass sensitivity arises as the propellant mass becomes a smaller fraction of system mass as the propellant atomic mass decreases.

The system dry mass, in general, decreased slightly with increasing specific impulse. The relative insensitivity of dry mass to specific impulse was primarily the result of the competing facts that the beam supply and thermal system mass increased with specific impulse (or system power) while the thruster, tankage, and support structure mass decreased with increasing specific impulse.

Because the mission parameters were fixed, the system power increased for each propellant by about 45 percent as the specific impulse was varied from its lowest to highest allowable values. In addition, the thrust was relatively insensitive to specific impulse with a maximum variation of about 7 percent for the data shown.

Figures 4 to 6 show that the number of thrusters, and their variation with specific impulse, were basically insensitive to propellant type. This situation arise due to the fact that at a fixed total voltage the output thrust of an individual thruster is insensitive to ion mass. For all the propellants it is seen that the number of thrusters decreased by slightly more than a factor of two over the range of attainable specific impulse.

Figures 4 to 6 show that the specific impulse strongly affects thrust system characteristics. For each propellant shown the thrust system dry mass, the propellant mass, and the number of thrusters decreased, while the power strongly increased, with increasing specific impulse.

Selection of an optimum specific impulse for a particular mission will depend upon the optimization criteria and cannot be inferred directly from the data of Figs. 4 to 6. For example, the payload mass was assumed herein to consist of the power source and other payload mass. While the overall payload mass increases with specific impulse, the non power source payload mass delivered to orbit could increase or decrease dependent on the specific mass assumed for the power source. Overall mission costs are also dependent upon assumptions and calculations beyond the scope of this paper. For example, the costs associated with the thrust system will undoubtedly decrease with increasing specific impulse while the power source cost will increase by an amount specific to power source type. The overall mission cost would also be influenced by the costs and revenues associated with the level of power on orbit and the concomitant other payload capabilities.

#### Propellant Type

The variation of system characteristics may be most clearly seen by cross plotting the data of Figs. 4 to 6. Figure 7 shows graphs of several parameters where the specific impulse for each propellant was arbitrarily selected as the lowest attainable value. The power requirements shown in Fig. 7 are then at their minimum values to perform the reference mission and can be seen to vary from about 225 kW for argon to 92 kW for mercury. In all cases the system mass increased with propellant mass

even though the system dry mass showed the opposite effect.

### Thrust Area

Figure 8 shows the major effects due to the variation of thruster area. In this case the propellant mass is constant and the system power was constant to within about one-percent. The number of thrusters decreases as expected with increasing area and this caused a decrease in the system dry mass of about slightly over 25 percent.

### PMAC Concept

Figure 9 shows major system characteristics for the DC and AC PMAC concepts. Mercury thrusters operated at 2500 seconds was assumed in Fig. 9. It is first seen that the system power for the DC case was about 5 kW greater than for the AC system. This difference which is all dissipated power, arose because of the higher efficiency expected for the AC system (Table III). The major impact of the efficiency difference between the AC and DC systems was to increase the required radiator area from about 14 to 25 m<sup>2</sup>. For a thrust system which is designed to fit within the shuttle envelope, this increase in radiator area may cause a substantial increase in the length of the thrust system. Single point designs of systems operating at about 100 kW indicate<sup>(21)</sup> that the length of the thrust system is driven by the required thermal radiator area. It is possible that other radiator concepts, such as those which radiate from both sides, could lessen the magnitude of the impact of power efficiency on system length.

### Mission Characteristics

The characteristics of electric propulsion systems are often plotted as functions of final mass or thrusting time with one of those parameters being an output variable. Equation (1) shows that the system thrust, which subsequently defines the system, may be specified by the rate of final mass to thrusting time. Use of that ratio allows convenient plotting of system characteristics for a very broad mission class.

Figure 10 shows major system parameters as a function of the ratio from Eq. (1). For reference the baseline mission used in the paper is shown by the arrows on Fig. 10. It is seen that all the major system parameters vary in a linear fashion with the mass/time ratio. This feature allows reasonable predictions of propulsion system characteristics to be rapidly estimated for a very wide range of missions.

### Concluding Remarks

A computer program was developed to allow rapid use of a methodology<sup>(14)</sup> to define the characteristics of electric propulsion systems for a broad range of geocentric missions. Overall system properties such as input power, dry mass, and propellant mass were presented for a wide range of assumed properties and approaches used for system elements. Technology parameters evaluated included thruster total accelerating voltage, specific impulse, pro-

pellant type, thruster beam area, and both AC and DC power systems. The impacts of technology parameter properties on overall system characteristics was shown to be quite significant in many cases. For example, variation of the specific impulse over the allowable range could change the overall system mass and the number of thrusters required by as much as a factor of two or more. The influence of the variation of mission trip time and final mass was conveniently displayed as a function of a single parameter.

The data presented herein should be useful in providing both direction for technology emphasis and preliminary estimates of the characteristics of electric propulsion systems.

### Acknowledgment

The author greatly acknowledges the efforts of W. F. Ford of the Lewis Research Center in developing the computer program which enabled rapid and accurate calculation of the data presented in this paper.

### References

1. Knight, R. M., "Planned Flight Test of a Mercury Ion Auxiliary Propulsion System. Part II - Integration with Host Spacecraft," AIAA Paper 78-647-II, Apr. 1978.
2. "30-Centimeter Ion Thrust Subsystem Design Manual," NASA TM-79191, 1979.
3. Kerslake, W. R. and Banks, B. A., "Evolution of the 1-lb Mercury Ion Thruster Subsystem," AIAA Paper 78-711B, Apr. 1978.
4. Hudson, W. R., "NASA Electric Propulsion Program," AIAA Paper 78-711, Apr. 1978.
5. Birner, W., Krulle, G., and Savary, M., "RIT-10 System Testing with Reference to a Flight Experiment," AIAA Paper 78-679, Apr. 1978.
6. Kuroda, Y., "Overview of the Electric Propulsion Program in Japan," AIAA Paper 78-715, Apr. 1978.
7. Bekey, I., "Big Comsats for Big Jobs at Low User Cost," *Astronautics and Aeronautics*, Vol. 17, Feb. 1979, pp. 42-56.
8. O'Neill, G. K., "Engineering a Space Manufacturing Center," *Astronautics and Aeronautics*, Vol. 14, Oct. 1976, pp. 20-28.
9. Fisher, J. H., "Space Transportation, Satellite Services, and Space Platforms," *Astronautics and Aeronautics*, Apr. 1979, pp. 42-51.
10. Ramsey, W. D., "12-Centimeter Magneto-Electrostatic Containment Argon/Xenon Ion Source Development," AIAA Paper 78-681, Apr. 1978.
11. Nakanishi, S. and Pawlik, E. V., "Experimental Investigation of a 1.5 Meter Diameter Kaufman Thruster," AIAA Paper 67-725, Sep. 1967.

12. Rawlin, V. K. and Hawkins, C. E., "Increased Capacities of the 30-cm Diameter Hg Ion Thruster," AIAA Paper 79-0910, May 1979.
13. Hansen, I. G., "Description of a 2.3 kW Power Transformer for Space Applications," NASA TM-79138, 1979.
14. Byers, D. C., Terdan, F. F., and Myers, I. T., "Primary Electric Propulsion for Future Space Missions," NASA TM-79141, 1979.
15. Cake, J. E., Sharp, G. R., Oglebay, J. C., Shaker, F. J. and Zavesky, R. J., "Modular Thrust Subsystem Approaches to Solar Electric Propulsion Module Design," AIAA Paper 76-1062, Nov. 1976.
16. Hawthorne, E. I., Weisman, Y. C., Frisman, N., Benson, G. C., McGrath, R. J., Martinelli, R. M., Linsenhardt, T. L., and Beattie, J. R., "Extended Performance Solar Electric Propulsion Thrust System Study, Vol. III, Tradeoff Studies of Alternate Thrust System Configurations," Hughes Research Labs., Malibu, CA, Sep. 1977. (NASA CR-135281-Vol-3).
17. Sovey, J. S., "A 30-cm Diameter Argon Ion Source," AIAA Paper 76-1017, Nov. 1976.
18. Byers, D. C., and Rawlin, V. K., "Critical Elements of Electron-Bombardment Propulsion for Large Space Systems," Journal of Spacecraft and Rockets, Vol. 14, Nov. 1977, pp. 648-654.
19. Rawlin, V. K., "Reduced Power Processor Requirements for the 30-cm Diameter Hg Ion Thruster," Paper to be presented at the AIAA/DGLR 14th International Electric Propulsion Conference, Oct. 30-Nov. 1, 1979.
20. Cady, E. C., private communication, McDonnell Douglas Astronautics Co., Huntington Beach, CA, 1975.
21. Silva, T. H. and Byers, D. C., "Nuclear Electric System Utilization for Earth Orbital Transfer of Large Spacecraft Structures," Paper to be presented at the AIAA/DGLR 14th International Electric Propulsion Conference, Oct. 30-Nov. 1, 1979.

TABLE I. - THRUSTER PERFORMANCE PARAMETERS WITH  
VARIOUS PROPELLANTS

Propellant	Propellant mass, M AMU	Propellant utilization efficiency, $\eta_U$	Thrust loss factor, $\gamma$	Power per beam ampere, $\epsilon_V$ , W/A
Mercury	200.6	0.95	0.95	150
Xenon	131.3	.95	<sup>a</sup> 0.95	183
Krypton	83.8	.9	<sup>a</sup> 0.95	220
Argon	39.9	.8	<sup>a</sup> 0.95	250

<sup>a</sup>Beam divergence loss contribution to  $\gamma$  taken from data with mercury propellant.

TABLE II. - SUMMARY OF PMAC MASSES

	DC		AC	
	Individual	Total	Individual	Total
<b>Thrust module</b>				
Beam supply	$M_B \approx 2.5 P_B^{3/4} + 1.8 P_B^{1/2} + 0.1 P_B + 7.6$	$N M_B$	$M_B \approx 0.12 P_B + 0.32 P_B^{2/3} + 0.18 P_B^{1/2}$	$N M_B$
Discharge supply	$M_D \approx 2.5 P_D^{3/4} + 1.8 P_D^{1/2} + 0.1 P_D + 3$	$N M_D$	$M_D$	$N M_D$
Low voltage supply	$M_{LO} = 8$	$N M_{LO}$	$M_{LO}$	$N M_{LO}$
<b>Interface module</b>				
Distribution inverter	$M_{DI} = P_{DI}^{3/4} + P_{DI}^{1/2} + 0.1 P_{DI} + 0.2$	$2 M_{DI}$		
House keeping converter	$M_C = P_C^{3/4} + P_C^{1/2} + 0.1 P_C + 0.9$	$2 M_C$	Identical to conventional approach	
Thrust system controller	$M_{TSC} = 4$	$2 M_{TSC}$		
Beam and discharge reconfig.	$M_{RU}$	$M_{RU} \approx 0.15 P_{RU}$	$M_{RU} = 3.5 P_{RU}^{3/4} + 2.3 P_{RU}^{1/2}$	

TABLE III. - SUMMARY OF PMAC DISSIPATED POWDERS

	DC	AC		
	Individual	Total	Individual	Total
<b>Thrust module</b>				
Beam supply	$P_{LB} \sim \frac{7}{93} P_B N'' P_B$		$P_{LB} \sim \frac{1}{49} P_B N'' P_B$	
Discharge supply	$P_{LD} \sim \frac{3}{22} P_D N'' P_D$		Identical to conventional approach	
Low voltage supply	$P_{LO} \sim 0.03 N'(0.03)$		Identical to conventional approach	
<b>Interface module</b>				
Distribution inverter	$P_{LDI} \sim \frac{1}{9} P_D$		Identical to conventional approach	
House keeping converter	$P_{LC} \sim \frac{1}{9} P_C$		Identical to conventional approach	
Thrust system controller	$P_{LTSC} \sim 0.15$		Identical to conventional approach	
Beam and discharge reconfig.	$P_{LRU} \sim \frac{N''}{199} P_{RU}$		$P_{LRU} \sim \frac{1}{99} P_{RU}$	

TABLE IV. - INPUT ASSUMPTIONS FOR CALCULATIONS

Variable evaluated	Case							
	I Total accel. voltage	II Specific impulse	III Specific impulse	IV Specific impulse	V Propellant	VI Area	VII PMAC type	VIII Mission parameters
Mission parameters								
Final mass, kg	$10^4$	$10^4$	$10^4$	$10^4$	$10^4$	$10^4$	$10^4$	NA
Thrusting time, days	150	150	150	150	150	150	150	NA
Mission velocity, m-sec <sup>-1</sup>	$6 \cdot 10^3$	$6 \cdot 10^3$	$6 \cdot 10^3$	$6 \cdot 10^3$	$6 \cdot 10^3$	$6 \cdot 10^3$	$6 \cdot 10^3$	$6 \cdot 10^3$
Thrust module								
Specific impulse, sec	$2 \cdot 10^3$	NA <sup>a</sup>	NA	NA	NA	$2.5 \cdot 10^3$	$2.5 \cdot 10^3$	$2.5 \cdot 10^3$
Propellant	Hg	Hg	Xe	Ar	NA	Hg	Hg	Hg
Thruster area, m <sup>2</sup>	0.1963	0.1963	0.1963	0.1963	0.1963	NA	0.1963	0.1963
Total accel. voltage, V	NA	$2 \cdot 10^3$						
Interface module								
PMAC type	DC	DC	DC	DC	DC	DC	NA	DC
Transmission line								
Length, m	100	100	100	100	100	100	100	100
Voltage, V	300	300	300	300	300	300	NA	300
Power type	DC	DC	DC	DC	DC	DC	NA	DC
Specific mass team, kg-w <sup>-1</sup>	0.02	0.02	0.02	0.02	0.02	0.02	0.02	0.02
F <sub>V</sub>	2.0	2.0	2.0	2.0	2.0	2.0	NA	2.0

<sup>a</sup>Not applicable.ORIGINAL PAGE IS  
OF POOR QUALITY

TABLE V. - ELEMENT CHARACTERISTICS

	Total accelerating voltage, $\Delta V$ , V		
	$1.5 \cdot 10^3$	$2.0 \cdot 10^3$	$2.5 \cdot 10^3$
Thrust module			
Initial number of operating thrusters, N''	17.96	9.4	5.69
Integral number of operating thrusters, N'	18.0	10	6.0
Total number of thrusters, N	20	12	8.0
Individual thruster full power thrust, N	0.302	0.577	0.95
Individual thruster full input power, kW	4.56	8.67	14.3
Total masses, kg			
Thrusters	406	245	163
Gimbals	139	83	55
Beam supplies	353	278	237
Discharge supplies	151	119	102
Low power supplies	160	96	64
Propellant distribution	20	12	8
Thermal control	241	234	230
Structure	169	102	68
Total thrust, N	5.43	5.43	5.43
Total mass, kg	1641	1169	928
Total input power, kW	89.7	89.0	88.7
Interface module			
Total masses, kg			
Distribution inverters	6	4	3
Controller	8	8	8
Converter	6	5	5
Reconfiguration unit	15	17	19
Propellant tank	34	34	34
Thermal control	22	19	18
Structure	212	193	184
Propellant	3578	3578	3578
Total mass, kg	3881	3859	3848
Total input power, kW	91.3	90.3	89.9
Transmission line			
Mass, kg	107	106	105
Input power, kW	96.7	95.6	95.1

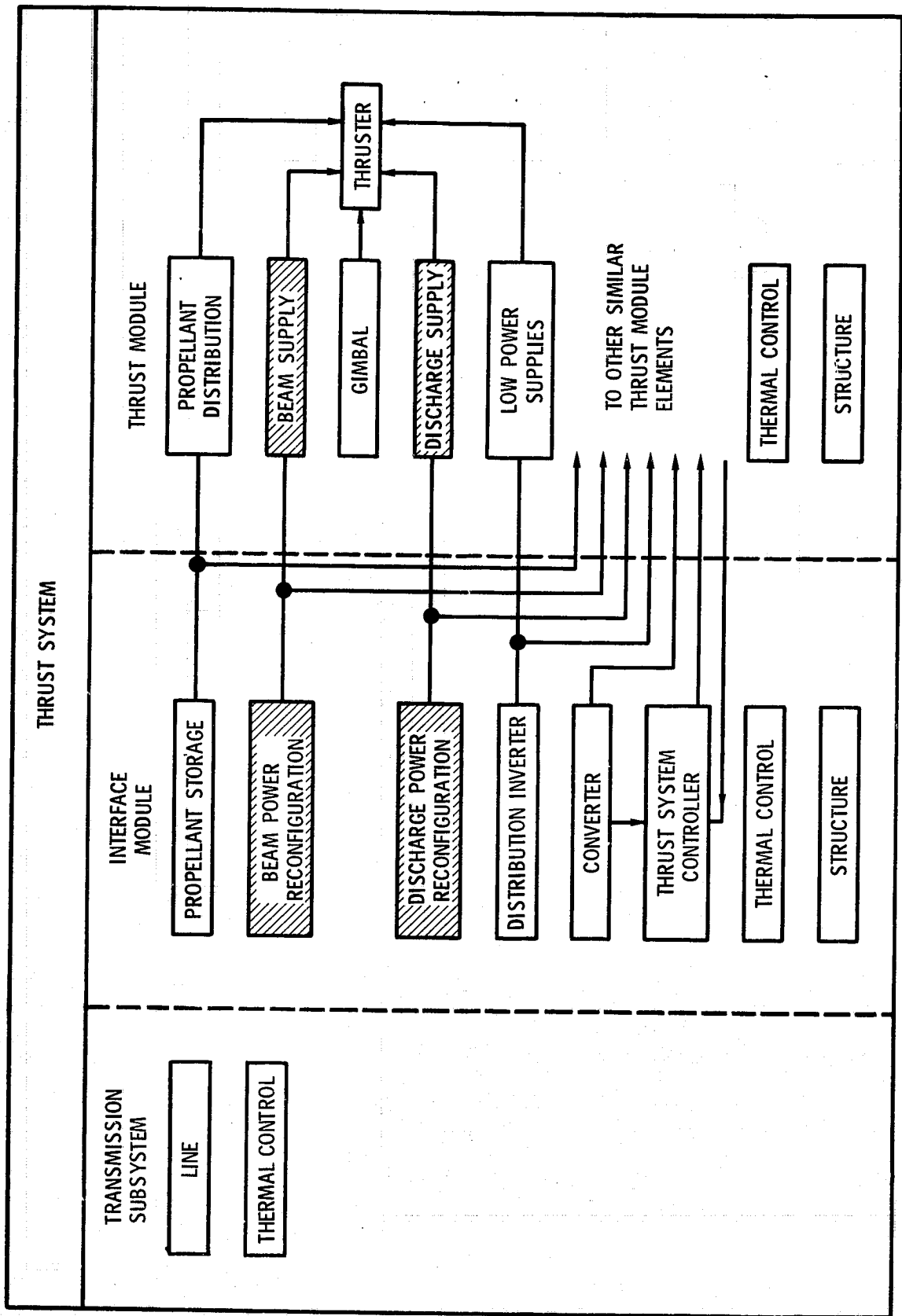


Figure 1. - Thrust system approach system approach.

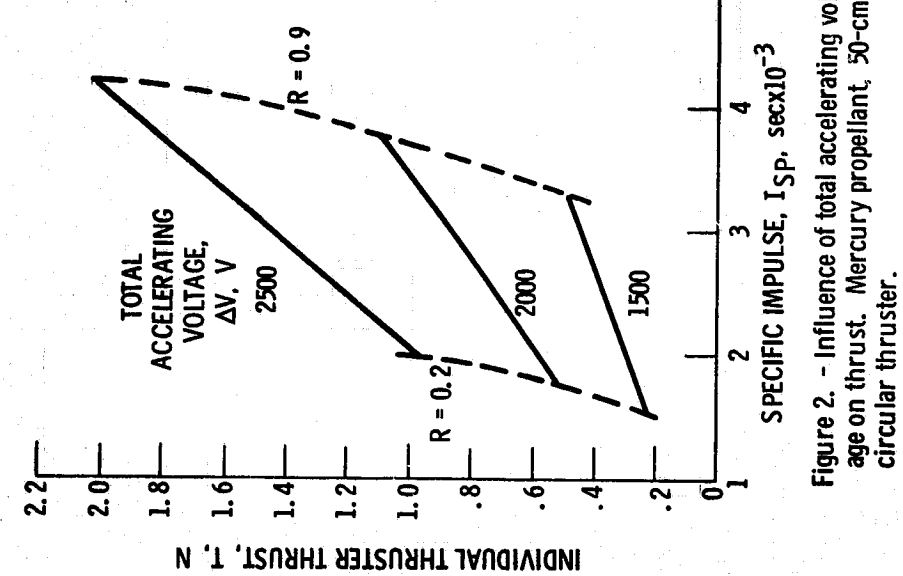


Figure 2. - Influence of total accelerating voltage on thrust. Mercury propellant, 50-cm circular thruster.

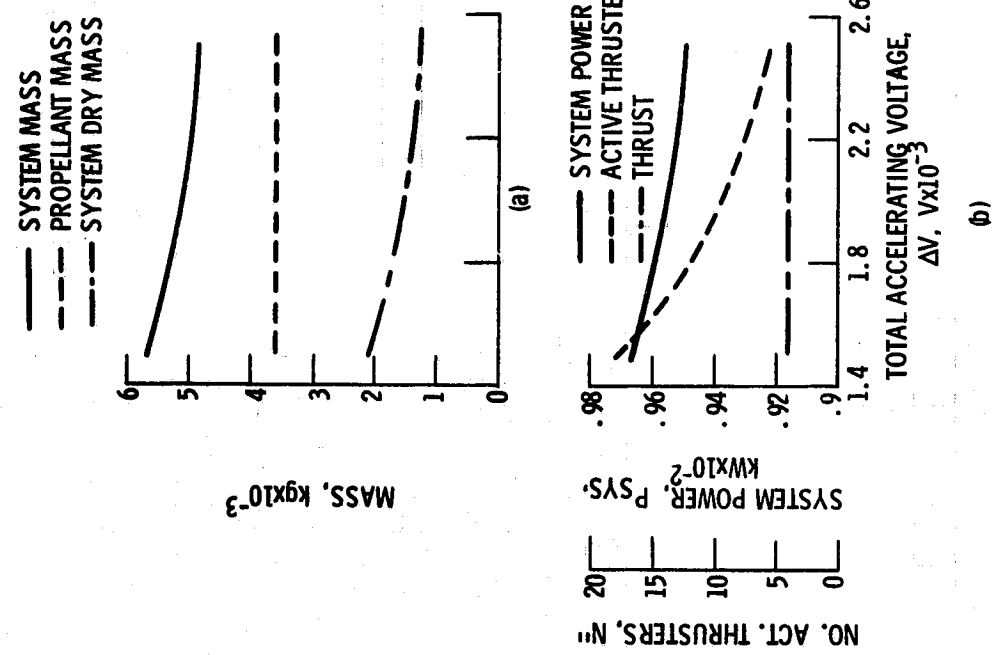
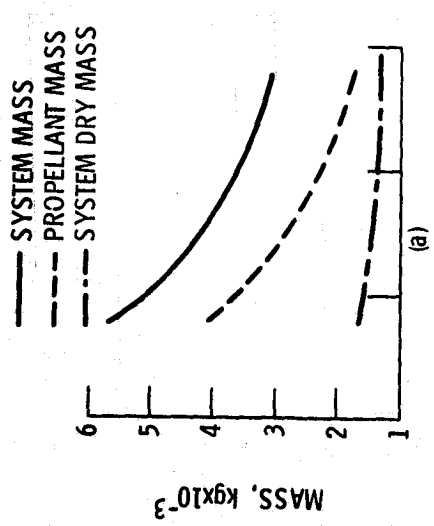
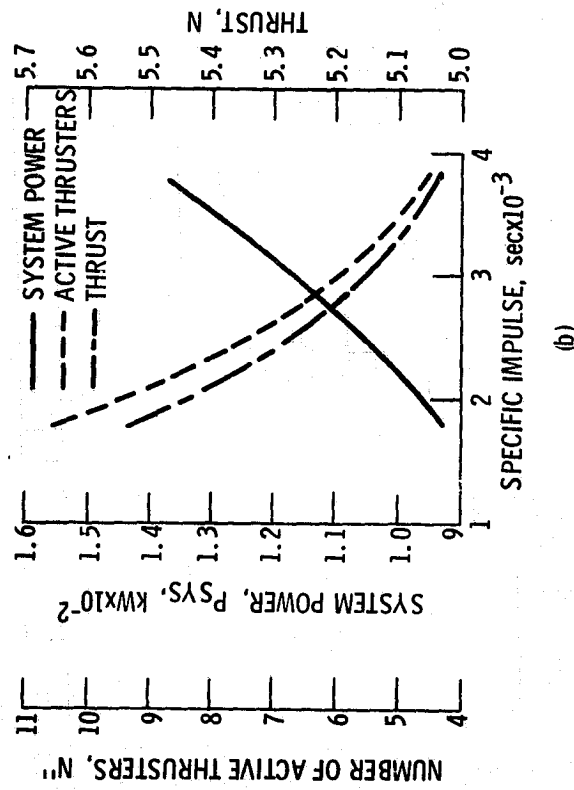


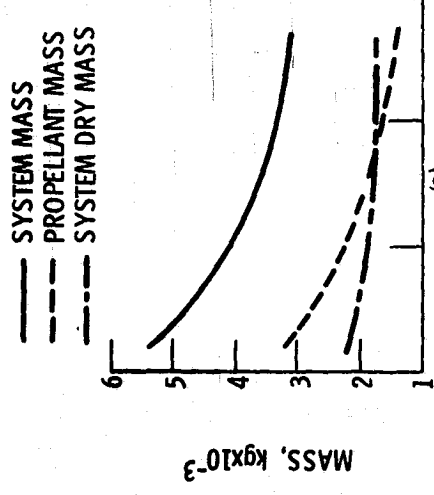
Figure 3. - Thrust system parameters as a function of total accelerating voltage. Case I, mercury propellant.



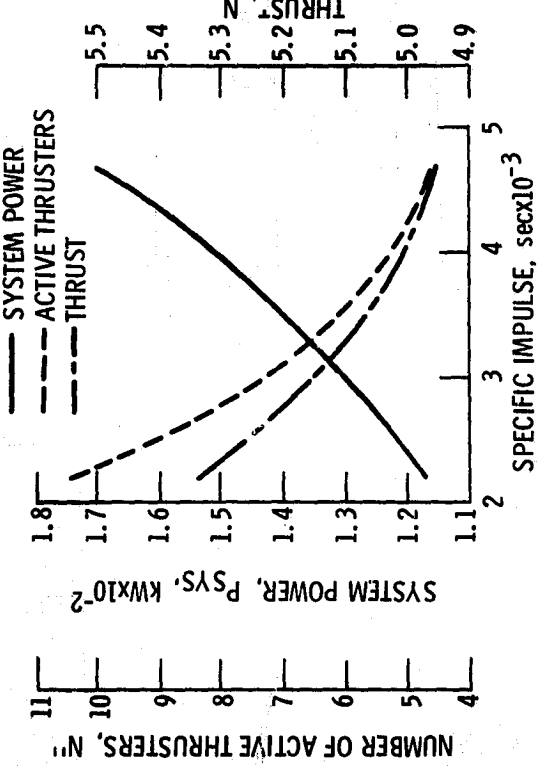
(a)



(b)



(a)



(b)

Figure 4. - Thrust system parameters as a function of specific impulse. Case II, mercury propellant.

Figure 5. - Thrust system parameters as a function of specific impulse. Case III xenon propellant.

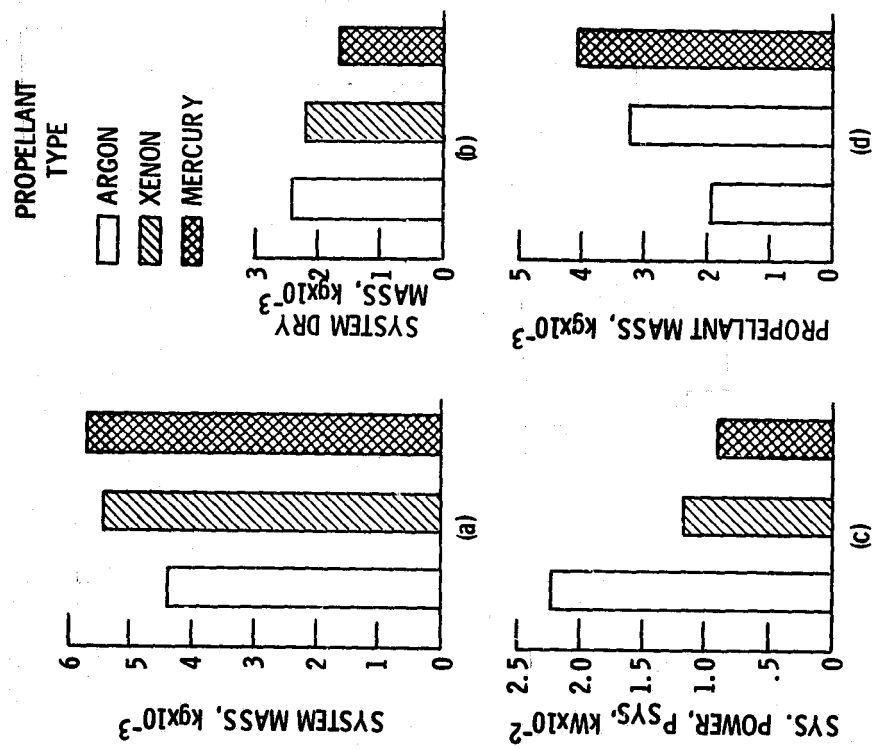


Figure 7. - Major system parameters as a function of propellant type. Case V.

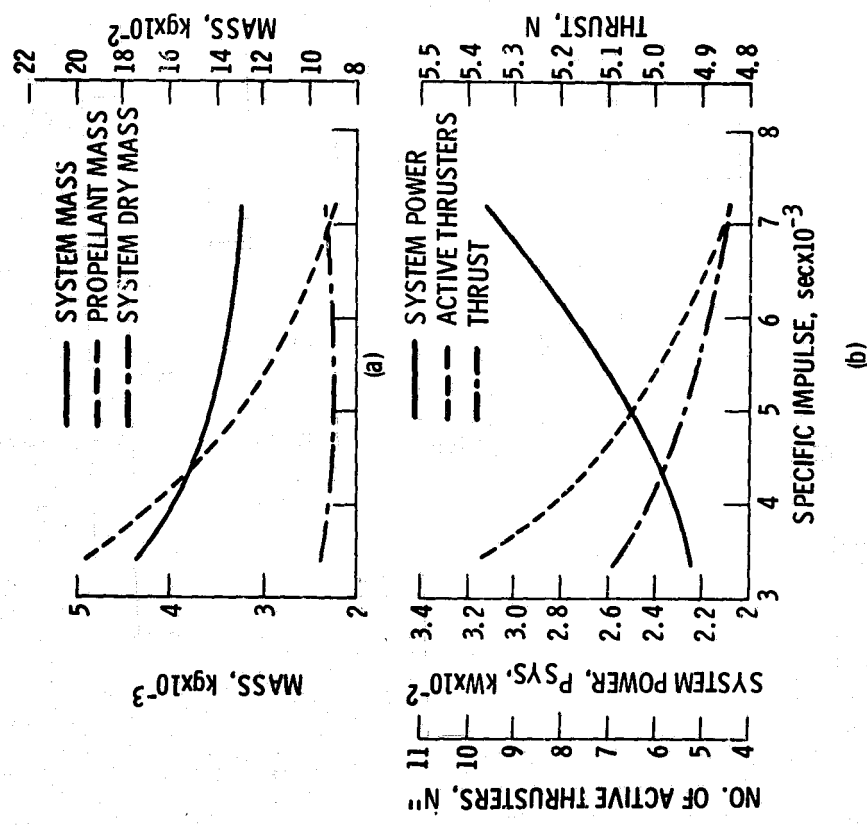


Figure 6. - Thrust system parameters as a function of specific impulse. Case IV, argon propellant.

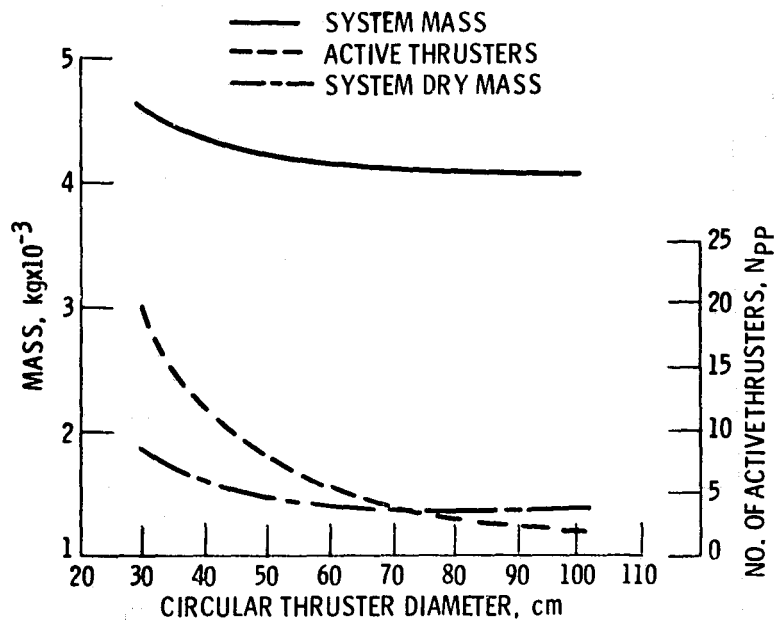


Figure 8. - Thrust system parameters as a function of active thruster diameter. Case VI mercury propellant.

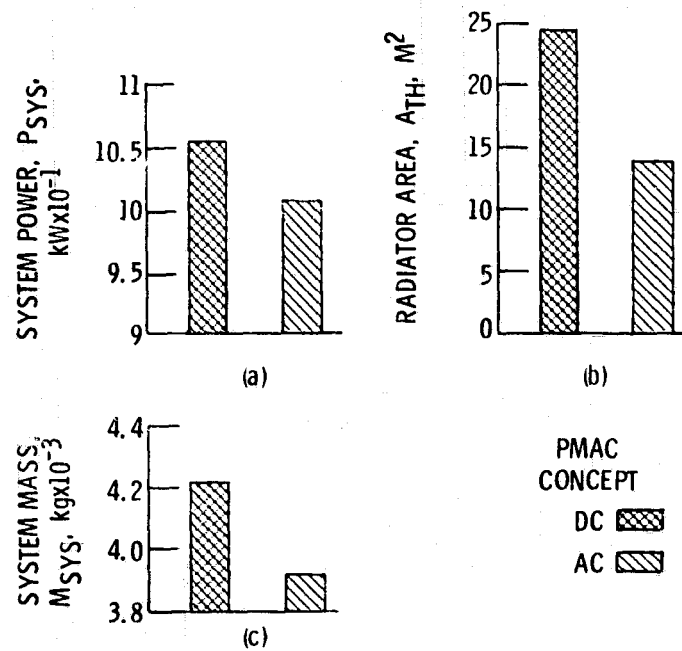
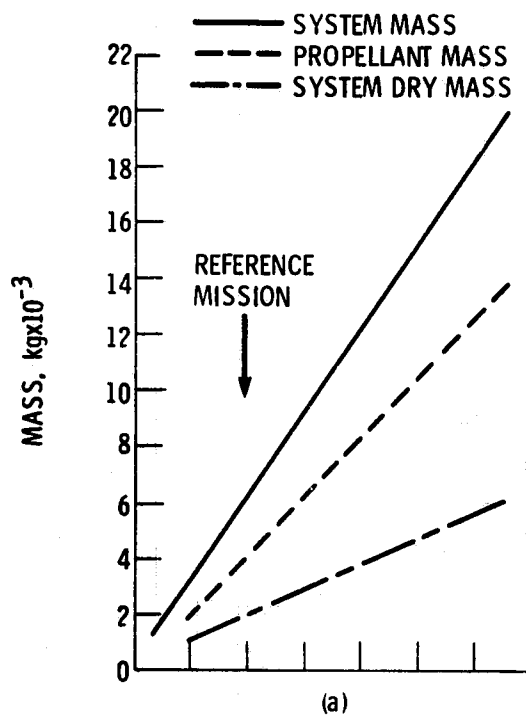
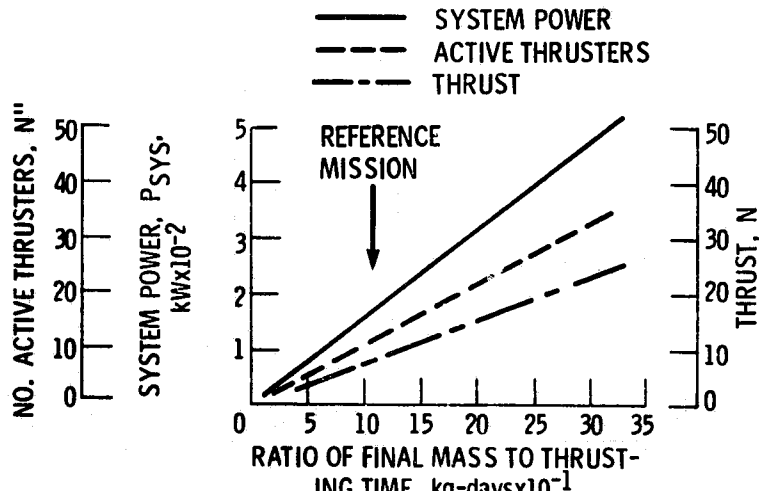


Figure 9. - Thruster system parameters as a function of  $P_{MAC}$  type. Case VI, mercury propellant. Specific impulse, 2500 sec.



(a)



(b)

Figure 10. - Thrust system parameters as a function of the ratio of final mass to thrusting time. Case VIII, mercury propellant, specific impulse, 2500 sec.